INSTITUTE OF PHYSICS PUBLISHING JOURNAL OF PHYSICS B: ATOMIC, MOLECULAR AND OPTICAL PHYSICS

J. Phys. B: At. Mol. Opt. Phys. **38** (2005) S309–S319 doi:10.1088/0953-4075/38/2/022

Zeros of Rydberg–Rydberg Föster interactions

Thad G Walker and Mark Saffman

Department of Physics, University of Wisconsin-Madison, Madison, WI 53706, USA

E-mail: tgwalker@wisc.edu

Received 30 June 2004
Published 5 January 2005
Online at stacks.iop.org/JPhysB/38/S309

Abstract

Rydberg states of atoms are of great current interest for quantum manipulation of mesoscopic samples of atoms. Long-range Rydberg–Rydberg interactions can inhibit multiple excitations of atoms under the appropriate conditions. These interactions are strongest when resonant collisional processes give rise to long-range C_3/R^3 interactions. We show in this paper that even under resonant conditions C_3 often vanishes so that care is required to realize full dipole blockade in micron-sized atom samples.

(Some figures in this article are in colour only in the electronic version)

1. Introduction

Rydberg–Rydberg interactions are very interesting for use in mesoscopic quantum manipulations. The extremely strong interactions between two Rydberg atoms have been proposed to entangle large numbers of atoms in a non-trivial manner using the phenomenon of blockade [1]. When a mesoscopic sample is illuminated with narrowband lasers tuned to a Rydberg state, only one atom at a time can be excited if the Rydberg–Rydberg interaction exceeds the linewidth of the laser–atom coupling. Therefore, the mesoscopic cloud of atoms behaves as an effective 2-level system, with the upper level being a single collective excitation.

In order to attain the strongest possible Rydberg blockade, it is desirable to operate under conditions where the Rydberg–Rydberg interaction is not the usual C_5/R^5 or C_6/R^6 van-der-Waals interactions, but instead is resonantly enhanced by 'Föster' processes [1, 2] such as

$$n\mathrm{s} + n\mathrm{s} \rightarrow n\mathrm{p} + (n-1)\mathrm{p} \tag{1}$$

that lead to isotropic C_3/R^3 long-range behaviour when the $n\mathrm{s} + n\mathrm{s}$ states are degenerate with the $n\mathrm{p} + (n-1)\mathrm{p}$ states. Dramatic enhancements of collisional interactions due to such resonant couplings have been demonstrated for Rydberg excitation in a magneto-optical trap [3]. The quantum nature of these types of interactions was recently used to resolve

molecules 12 nm apart in an organic solid [4]. Due to the high density of Rydberg states, there are typically many candidate levels for such Föster processes.

An important consideration for quantum information applications of Rydberg blockade is the size of cloud required. The spatial extent of the cloud must be small enough for excitation of a single atom anywhere in the cloud to block the excitation of every other atom in the cloud. Even with the great strength of Rydberg–Rydberg interactions, the required size of the clouds is likely to be less than 10 μm for fast (1 MHz) operations. Only recently have atom clouds of such small size been produced in the laboratory [5, 6]. Even in the case that sub-micron mesoscopic samples are realized experimentally, there are other applications of such samples that benefit from the sample being as large as possible. For example, we have recently proposed single-photon sources, single-photon detectors and quantum state transmission [7, 8] using mesoscopic Rydberg blockade. In these applications one would like the cloud to be many wavelengths in size in order that the diffraction limited light fields not occupy too large a solid angle. For this to be effective requires the blockade to operate over clouds of several microns in extent.

The purpose of this paper is to examine some issues that arise in the application of Föster processes to Rydberg blockade. In particular, when the quantum numbers for the states are of the form

$$nl + nl \rightarrow n'(l-1) + n''(l \pm 1) \tag{2}$$

we show that one or more of the $nl + nl$ states have $C_3 = 0$. These 'Föster zero' states then only exhibit the usual van-der-Waals long-range behaviour and will therefore set limits on the attainable cloud sizes for quantum manipulations using Rydberg blockade. Only when $l' = l'' = l + 1$ are there no Föster zero states. Recent experiments [9, 10] have observed strong suppression of excitation in very large clouds that is strong evidence for blockade but do not address whether or not the blockade is complete as required for quantum information applications.

In the following, we first (section 2) present a more detailed background discussion of the importance of strong isotropic Rydberg–Rydberg interactions for quantum manipulations using Rydberg blockade. We then illustrate in section 3 how the Föster process accomplishes this. Section 4 presents the main result of this paper: for many possible Föster processes there exists a linear combination of atomic sublevels that have $C_3 = 0$. This result is extended to the important case of fine-structure interactions in section 5. We conclude with more implications of this work.

2. Background

The basic physics behind the Rydberg-blockade concept is illustrated in figure 1. Suppose we have two atoms in an atomic ground state a. We envision exciting the atoms to a Rydberg state r of energy E_r using a narrowband laser. As shown in the figure, excitation of one of the two atoms to the Rydberg state is allowed while excitation of the second atom is off-resonant and therefore suppressed. Addition of more atoms changes the effectiveness of this 'blockade' but does not change the basic physics of the situation. Excitation of more than one atom is energetically suppressed as long as the interaction between each pair of atoms in the ensemble exceeds the bandwidth of the laser–atom excitation. Neglecting spontaneous emission or other decohering effects, when subject to blockade and a continuous light field the atoms will undergo coherent Rabi oscillations between states $a + a$ and $a + r$.

To see how this process can be used to generate interesting entanglement, we simply imagine driving the atom pair in the $|aa\rangle$ state with a π pulse. The atoms will then be in a

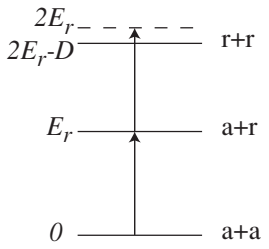

Figure 1. Energy levels for a pair of atoms being excited by a light field to Rydberg states. Excitation of one of the two atoms is resonantly favoured but two-atom excitations are off resonance by the dipole–dipole interaction energy D.

coherent superposition of states a and r

$$\psi(\pi) = \frac{-\mathrm{i}}{\sqrt{2}}\left(|ar\rangle + |ra\rangle\right) \tag{3}$$

that cannot be written as a product of two individual wavefunctions and is therefore entangled. To avoid the inevitable decoherence of the unstable Rydberg state, the entanglement can be usefully transferred to a second ground state b with a π-pulse from a second laser tuned to the $r \rightarrow b$ transition. Again, this concept can be extended to a collection of N atoms without loss of generality. The final wavefunction is a symmetric entangled superposition of $N-1$ atoms in state a and one atom in state b.

There are several intriguing characteristics of this process. First, the entanglement is generated between the internal states of the atom; any motion of the atom is unimportant. This means that it is not necessary for the atoms to be localized in the ground state of a confining potential, so the method does not require coherence of the external degrees of freedom of the atoms. There is also no motional constraint on the speed at which the process can occur. Second, the value of the Rydberg–Rydberg interaction $D(R)$ is not important to first order, as long as it is much larger than the bandwidth γ of the light-atom interaction. This implies that the atoms can be at random distances R from each other, as long as $D(R) \gg \gamma$. Finally, since the blockade mechanism suppresses excitation of multiple Rydberg atoms, the atoms never actually experience the strong Rydberg–Rydberg forces, avoiding heating.

Key to the entanglement process is the requirement that the Rydberg–Rydberg frequency shift be large compared to the bandwidth of the light-atom interaction. If this is violated, the fidelity of the entanglement operations will be compromised. In a mesoscopic sample, insufficient blockade in any possible excitation channel is sufficient to cause production of multiple excited atoms. We now examine the Rydberg–Rydberg interactions to see under what conditions this will be problematic.

3. Föster process

We wish to consider the interactions between two like Rydberg atoms that lead to blockade. Normally, in the absence of an external electric field these interactions are of the van-der-Waals forms $1/R^5$ or $1/R^6$. Since an electric field mixes states of opposite parity together, a Rydberg atom can have a permanent dipole moment $\langle \mathbf{p} \rangle = -e\langle \mathbf{r} \rangle$ of magnitude as large as $-n^2 e a_0$, where e is the electronic charge and a_0 the Bohr radius, leading to a much stronger and longer range $1/R^3$ interaction. This is illustrated in figure 2. Focusing on the 50d state, for fields above 5 V cm^{-1} the energy becomes linear in the field. The slope of the energy versus field

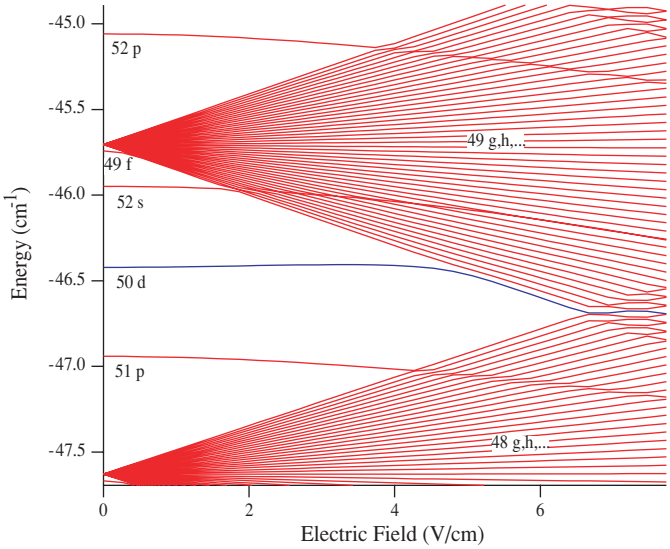

Figure 2. Stark map for states near $n = 50$ for Rb. At electric fields around 5–6 V cm^{-1}, the atom acquires a large permanent dipole moment, oriented in space along the applied field.

gives the dipole moment, 3300 ea_0 in this case. The interaction between two such atoms A and B is the familiar dipole–dipole form

$$V_{DD} = \frac{1}{R^3}(3\mathbf{p}_A \cdot \hat{\mathbf{R}}\hat{\mathbf{R}} \cdot \mathbf{p}_B - \mathbf{p}_A \cdot \mathbf{p}_B) = \frac{p^2}{R^3}(3\cos^2\theta - 1) \tag{4}$$

where θ is the angle between the interatomic separation $\mathbf{R}$ and the electric field $F\hat{\mathbf{z}}$. The fact that $p \sim n^2 ea_0$ makes this interaction huge for two Rydberg states. However, because the dipoles are oriented in space by the applied field, the interaction vanishes at $\theta = \cos^{-1}\sqrt{1/3} = 54.7^\circ$. This is undesirable for dipole blockade because it allows for excitation of Rydberg atom pairs located at this angle with respect to each other.

Even in the absence of a mixing electric field, it is possible to have an isotropic Rydberg atom–atom interaction of comparable strength to V_{DD} if there is a degeneracy in the energy-level spectrum for a pair of atoms. For example, inspection of figure 3 shows that the 50s state of rubidium (Rb) is nearly symmetrically placed between the 49p and 50p states. This means that the 50s+50s state of a Rydberg atom pair is nearly degenerate with the 49p + 50p state. Neglecting the influence of other nearby states, the eigenstates of the two-atom system are linear combinations of 50s+50s and 49p+50p, with energy shifts proportional to $1/R^3$. Using the methods described below, we find that the Rydberg–Rydberg potential energy curves are given by

$$U_\pm(R) = \frac{\delta}{2} \pm \sqrt{\frac{4U_3(R)^2}{3} + \frac{\delta^2}{4}} \tag{5}$$

where $U_3(R) = e^2\langle 50\mathrm{s}||r||50\mathrm{p}\rangle\langle 50\mathrm{s}||r||49\mathrm{p}\rangle/R^3 = 5.75 \times 10^3$ MHz μm$^3/R^3$ and the ss–pp energy defect is $\delta = E(49\mathrm{p}) + E(50\mathrm{p}) - 2E(50\mathrm{s}) = -3000$ MHz. Estimates similar to this have been previously presented by Protsenko *et al* [11].

A plot of $U_+(R)$ is shown in figure 4. It is isotropic (independent of θ), lacking the undesirable zeros of V_{DD} equation (4) . If there were perfect Föster degeneracy ($\delta = 0$) $U_+(R)$

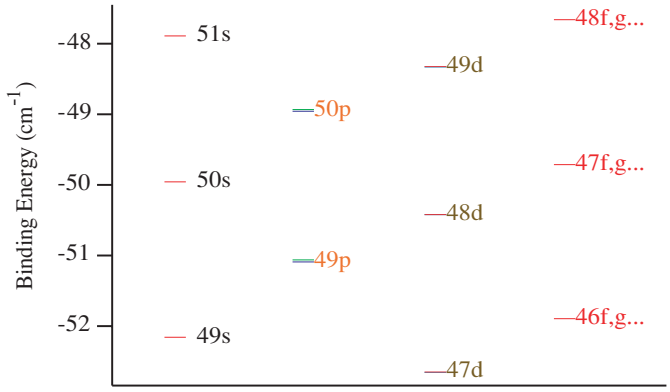

Figure 3. Energy levels for Rb near $n = 50$. The fine-structure splitting for the p-states is just discernable.

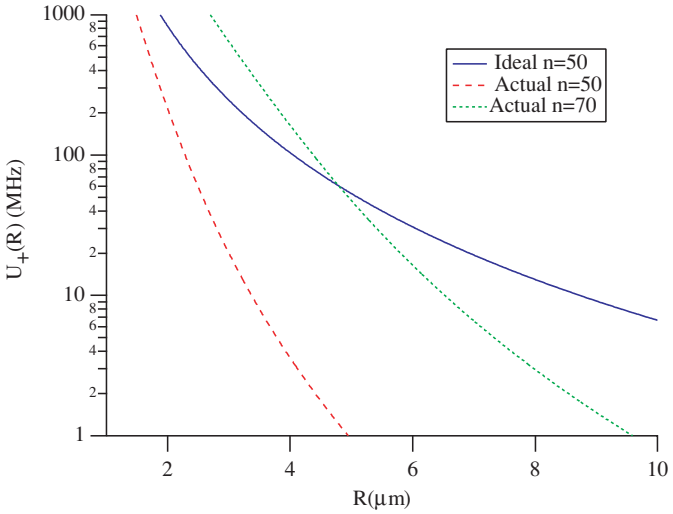

Figure 4. Isotropic dipole–dipole interaction for excitation to the Rb 50s state. The energy defect between the 50s+50s and 49p+50p states significantly reduces the interaction as compared to the ideal degenerate case. Going to larger n partially compensates for the non-zero energy defect.

would be of similar strength and range to V_{DD}. In the example given, $U_+(R)$ exceeds 10 MHz out to distances of 10 μm. This would be very promising for realizing dipole blockade in quite large, optically resolvable clouds. However, as illustrated in figure 4, the energy defect for real Rb atoms reduces the interaction strength substantially, becoming the usual van-der-Waals form $-4U_3(R)^2/3\delta$ at large distances.

An interesting possibility is to tune the energy defect to zero with an external electric field. In some cases it might be possible to do this using electric fields which are sufficiently weak that the s–p mixing would be small. However, it turns out that for Rb the quantum defects of the s- and p-states are such that the application of a small electric field increases the magnitude of δ, thus further reducing the Rydberg–Rydberg interaction strength. This is shown (for the 52s state) in figure 2.

The strength of the Rydberg–Rydberg interactions varies strongly with principal quantum number. The radial matrix elements scale as n^2, so U_3 scales as n^4. Since the energy defect δ scales as n^{-3}, the van-der-Waals interactions scale as $U_3^2/\delta \sim n^{11}$. Thus the range of the Rydberg blockade increases as roughly $n^{11/6}$, so that $n = 70$ has nearly twice the range as $n = 50$, as illustrated in figure 4. Increasing n comes with increased sensitivity to stray electric fields, black-body radiation and so forth. In practice, states up to $n \sim 100$ should be stable enough to perform fast quantum operations [12]. However, it would be preferable to find states with smaller energy defects and therefore larger range at smaller n.

Given the lack of perfect Föster resonances for the s-state, one should consider the possibility of Föster processes in other angular momentum states where the energy defects may be smaller (or more tunable) than they are for the s-states. This topic will be taken up in the following section.

Before proceeding, we should note that we have restricted our calculations to states that are nearly resonant. Other states, such as 51p+48p in the above example, have larger energy defects ($\delta = 12$ GHz for 51p+48p) and often much smaller matrix elements as well. Adding up many such states could (and should) be done in second-order perturbation theory and will alter the $1/R^6$ part of the potential somewhat but not change the overall conclusions. For the rest of this paper we will continue to neglect these other states. We will also neglect the $1/R^5$ quadrupole–quadrupole interactions, and assume no electric field mixing.

4. Föster zeros

Interesting new properties of the Föster process arise when we consider higher angular momentum states. For example, consider again the s- and p-states of Rb, but this time with laser excitation of the p-states, so that the relevant Föster degeneracy is, say, 50p+50p→50s+51s with an energy defect $\delta = 930$ MHz. Suppose also that the atoms are subject to linearly polarized light polarized along the laboratory $\hat{\mathbf{z}}$-axis. We shall show that there is no Föster-induced blockade for this situation. For simplicity, let us assume that two atoms A and B are aligned with $\hat{\mathbf{R}} = \hat{\mathbf{z}}$, with their states denoted $|(nlm)_A(nlm)_B\rangle$, m being the magnetic quantum number. In this case, consider the wavefunction

$$|\psi_0\rangle = \tfrac{1}{\sqrt{3}}|50\mathrm{p}1\ 50\mathrm{p}\bar{1}\rangle - \tfrac{1}{\sqrt{3}}|50\mathrm{p}0\ 50\mathrm{p}0\rangle + \tfrac{1}{\sqrt{3}}|50\mathrm{p}\bar{1}\ 50\mathrm{p}1\rangle \tag{6}$$

($\bar{1} = -1$) whose matrix element of V_{DD} is zero with the s + s states:

$$\langle 50\mathrm{s}\ 51\mathrm{s}|V_{DD}|\psi_0\rangle = 0 \tag{7}$$

and so the only long-range interaction will be a van-der-Waals interaction with the comparatively far off-resonant d+d and d+s states. Note that $|\psi_0\rangle$ is strongly coupled to the light through its $|50\mathrm{p}0\ 50\mathrm{p}0\rangle$ part. With strong light coupling and weak dipole–dipole coupling, we conclude that the Rb p-states will not experience long-range dipole blockade. These conclusions are not changed when $\hat{\mathbf{R}}$ is rotated away from $\hat{\mathbf{z}}$. If one takes the quantization axis along $\hat{\mathbf{R}}$ then $|\psi_0\rangle$ stays of the same form, but each of the three parts of $|\psi_0\rangle$ will contribute to the light-atom interaction. For the rest of the paper we shall take the quantization axis for the atomic basis states to be along $\hat{\mathbf{R}}$.

Another very interesting possibility from figure 3 is the nearly degenerate combination 48d+48d→50p+46f with an energy defect of only 110 MHz (neglecting fine structure for now). This has the potential for much stronger Föster interactions at large distance as compared to the s+s states. In this case there is also a wavefunction with zero coupling via V_{DD} to the p+f manifold:

$$|\psi_0\rangle = \frac{1}{\sqrt{107}}|48\mathrm{d}0\ 48\mathrm{d}0\} + \sqrt{\frac{8}{107}}|48\mathrm{d}1\ 48\mathrm{d}\bar{1}\} + \sqrt{\frac{98}{107}}|48\mathrm{d}2\ 48\mathrm{d}\bar{2}\} \tag{8}$$

where interchange-symmetric kets are defined in terms of the quantum numbers $A = n_A l_A m_A$ of the individual atoms as $|AB\} = (|AB\rangle + |BA\rangle)/\sqrt{2 + 2\delta_{m_A m_B}}$, and $\bar{m} = -m$. We shall label such states as Föster zero states.

Whereas the Föster zero state of equation (6) can be deduced in a straightforward way essentially by inspection once the matrix elements of s+s with the three p+p combinations are calculated, the d+d Föster zero state of equation (8) is more subtle since its matrix elements with each of the three $|pm\ f\bar{m}\}$ states must vanish. Thus we now discuss in more generality the conditions for Föster zero states to exist for the process

$$nl_0 + nl_0 \to n'l_1 + n''l_2. \tag{9}$$

We will assume without loss of generality that $l_1 \leqslant l_2$.

The Föster zero state, if it exists, is written as a linear combination $|\psi_0\rangle = \sum_{m_0=0}^{l_0} c(m_0)|l_0 m_0\, l_0 \bar{m}_0\}$, so the condition $V_{DD}|\psi_0\rangle = 0$ gives

$$\sum_{m_0=0}^{l_0} c(m_0)\{l_1 m\, l_2 \bar{m}|V_{DD}|l_0 m_0\, l_0 \bar{m}_0\} = 0 \tag{10}$$

which is effectively a generalization of equation (7) to the case where there are multiple possible final states. There are three cases of interest. For $l_1 = l_0 - 1$ and $l_2 = l_0 + 1$ (of which d+d→p+f is an example) there are $2l_1 + 1 = 2l_0 - 1$ equations in the $l_0 + 1$ unknowns $c(m_0)$. But the reflection symmetry $\{l_0 m_0\, l_0 \bar{m}_0|V_{DD}|l_1 m\, l_2 \bar{m}\} = \{l_0 m_0\, l_0 \bar{m}_0|V_{DD}|l_1 \bar{m}\, l_2 m\}$ means that $2l_1$ of the equations are the same, leaving l_0 equations in $l_0 + 1$ unknowns and therefore a solution exists. For the case $l_1 = l_2 = l_0 - 1$ the same argument holds. The final case, with $l_1 = l_2 = l_0 + 1$, has equation (10) with $l_0 + 2$ equations in $l_0 + 1$ unknowns and therefore no Föster zero state.

These results can also be understood from the point of view of the molecular symmetries of the problem. Following the analysis of Marinescu [13], the Föster zero states have the molecular symmetries ${}^3\Sigma_u^+$ and ${}^1\Sigma_g^+$ depending on their triplet or singlet spin character. For $l_1 \neq l_2$, the orbital exchange-symmetric kets as defined above are not eigenstates of the operator σ_v that reflects the wavefunction about a plane containing the interatomic axis. Taking into account this symmetry, we define kets

$$|l_1 m\, l_2 \bar{m}) = |l_1 m\, l_2 \bar{m}\rangle + \beta|l_2 \bar{m}\, l_1 m\rangle + \lambda|l_1 \bar{m}\, l_2 m\rangle + \lambda\beta|l_2 m\, l_1 \bar{m}\rangle \tag{11}$$

which have molecular parity (g, u) if $p = (\bar{1})^{l_1+l_2+S}\beta = (1, \bar{1})$ and reflection symmetry eigenvalues $\sigma = \beta\lambda$, giving rise to states of traditional molecular designation ${}^{2S+1}\Sigma_{g,u}^{\sigma}$. Considering triplet states, and assuming $l_1 < l_2$, there are $l_1 + 1\lambda = \beta = 1\,{}^3\Sigma_u^+$ states, $l_1 + 1\lambda = 1, \beta = \bar{1}\,{}^3\Sigma_g^-$ states, $l_1\lambda = \bar{1}, \beta = 1\,{}^3\Sigma_u^-$ states, and $l_1\lambda = \beta = \bar{1}\,{}^3\Sigma_g^+$ states. Thus for the d+d→p+f problem, there are three ${}^3\Sigma_u^+$ states with d+d character but only two of p+f character. Therefore, it is always possible to find a linear combination of the three ${}^3\Sigma_u^+$ d+d states that has zero coupling to the two p+f ${}^3\Sigma_u^+$ states. The reasoning is identical for the ${}^1\Sigma_g^+$ symmetry.

To summarize, the isotropic C_3/R^3 dipole–dipole interaction generated by the Föster process $l_0 + l_0 \to l_1 + l_2$ will have states with $C_3 = 0$ unless $l_1 = l_2 = l_0 + 1$.

The above analysis has emphasized the ${}^3\Sigma_u^+$ and ${}^1\Sigma_g^+$ states that are degenerate in the absence of overlap. Similar reasoning shows that for the case $l_1 = l_0 - 1, l_2 = l_0 + 1$ the ${}^3\Sigma_g^-$ and ${}^1\Sigma_u^-$ states have no Föster zeros, nor do states of $\Lambda > 0$. In general, all of these states are coupled to the light field, but the ${}^3\Sigma_u^+$ and ${}^1\Sigma_g^+$ states destroy the complete blockade.

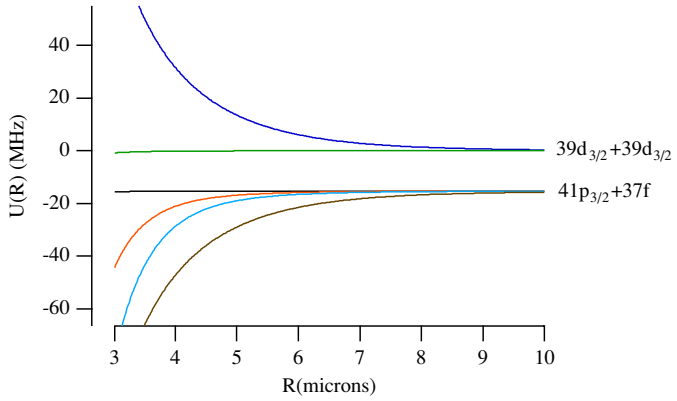

Figure 5. Long-range $0_{gu}^{\pm}$ potential curves near the 39d+39d asymptote of Rb_2. The nearly flat curve coming from the 39d+39d asymptote implies suppressed dipole blockade.

5. Fine-structure effects

In general, the fine-structure interaction cannot be neglected. At $n = 50$ the Rb p-state fine-structure splitting is about 800 MHz and the d splitting is 100 MHz, so that at micron-scale distances there will be strong fine-structure mixing by the dipole–dipole interaction. At long enough range, where the dipole–dipole interaction is smaller than the fine-structure splitting, we can use the same type of arguments as above to analyse the problem.

Let us consider the Föster process

$$l_0 j_0 + l_0 j_0 \rightarrow l_1 j_1 + l_2 j_2. \tag{12}$$

We are mostly interested in states with total $m_j = 0$. As before, the $l_0 j_0 + l_0 j_0$ states are symmetric linear combinations $|l_0 j_0 m\, l_0 j_0 \bar{m}\}$. For alkali atoms with half-integer j there are $j + 1/2$ such states. On the other hand, there are (assuming $j_1 \leqslant j_2$) $2j_1 + 1 | l_1 j_1 m_0\, l_2 j_2 \bar{m}_0\}$ states. Half of these are removed from consideration due to the

$$\{l_0 j_0 m_0\, l_0 j_0 \bar{m}_0 | V_{DD} | l_1 j_1 m\, l_2 j_2 \bar{m}\} = \{l_0 j_0 m_0\, l_0 j_0 \bar{m}_0 | V_{DD} | l_1 j_1 \bar{m}\, l_2 j_2 m\}$$

symmetry. Thus the system of equations for the Föster zero amplitudes $c(m)$ has $j + 1/2$ equations in $j_1 + 1/2$ unknowns. A normalizable solution will exist only for $j_1 < j$. It follows that potential Föster processes such as $n\mathrm{d}_{3/2} + n\mathrm{d}_{3/2} \rightarrow (n+2)\mathrm{p}_{1/2} + (n-2)\mathrm{f}_{5/2}$ will have zeros.

The inclusion of fine structure brings new possibilities, however, since states of different l can have the same value of j. For example,

$$n\mathrm{d}_{3/2} + n\mathrm{d}_{3/2} \rightarrow (n+2)\mathrm{p}_{3/2} + (n-2)\mathrm{f}_{5/2} \tag{13}$$

has an energy defect of only -15 MHz at $n = 39$ and should not have any Föster zeros. The Hamiltonian matrix has the structure

$$H = \begin{pmatrix} \mathrm{diag}(0) & WU_3(R) \\ WU_3(R) & \mathrm{diag}(\delta) \end{pmatrix} \tag{14}$$

where the interaction submatrix

$$W = \begin{pmatrix} \frac{-4}{25}\sqrt{\frac{2}{3}} & 0 & 0 & \frac{4}{25}\sqrt{\frac{2}{3}} \\ \frac{8}{25}\sqrt{\frac{2}{3}} & \frac{4}{75} & \frac{-4}{75} & \frac{-8}{25}\sqrt{\frac{2}{3}} \end{pmatrix} \tag{15}$$

and $U_3(R) = e^2\langle 39\mathrm{d}||r||41\mathrm{p}\rangle\langle 39\mathrm{d}||r||37\mathrm{f}\rangle/R^3 = 2940$ MHz $\mu\mathrm{m}^3/R^3$. For $\delta = 0$, the eigenvalues of H corresponding to the d+d states are $(\pm 4\sqrt{31 \pm \sqrt{937}}/75)U_3(R)$. Two of the eigenvalues are quite small ($\pm 0.033U_3(R)$), leading to poor Rydberg blockade. The potential curves for $\delta = -15$ MHz are shown in figure 5. The nearly flat potential shows that while there are no Föster zeros for this case, the Rydberg blockade is still strongly suppressed at large distances even though the energy defect is very small. Even in the presence of fine structure, the blockade is still poor if $l_1 < l_0$.

6. Conclusions

The primary result of this paper is that the very long-range C_3/R^3 interactions produced by resonances $nl + nl \rightarrow n'l_1 + n''l_2$ have states with $C_3 = 0$ unless $l_1 = l_2 = l + 1$. This strongly reduces the number of possibilities for attaining high fidelity dipole-blockade in mesoscopic atom samples. One solution is to rely instead on quadrupole–quadrupole ($1/R^5$) or second-order dipole–dipole ($1/R^6$) interactions to achieve blockade at high values of n. As pointed out recently by the Connecticut group [14, 9] the interactions under these conditions can be quite strong.

Another possibility for attaining strong dipole blockade is to tune $l_1 = l_2 = l + 1$ resonances with an electric field. For example, the great sensitivity of f states to electric fields can tune d+d→f+f into resonance at modest fields. At resonance, the long-range potentials for this case are $\pm 0.336U_3$, $\pm 0.227U_3$, $\pm 0.158U_3$ and thus should lead to quite strong Rydberg blockade at long range.

An important topic for further study is the sensitivity of the Föster zeros to electric fields. If the Stark splitting of the p or d magnetic sublevels is greater than U_3, we would expect the zeros to no longer be present. However, an important question is whether the Rydberg–Rydberg interaction becomes anisotropic in this case, since the atoms would also acquire a permanent, spatially oriented dipole moment.

Acknowledgments

The authors recognize very helpful conversations with other members of the Wisconsin AMO Physics group, and with C Goebel and R Cote. This work was supported by the National Science Foundation, NASA, and the Army Research Office.

Appendix

A.1 Calculation of dipole–dipole matrix elements

Let l, l_1, and $l_2 \geqslant l_1$ be the angular momenta involved in the Föster process

$$nl + nl \rightarrow n'l_1 + n''l_2. \tag{A.1}$$

Since the dipole–dipole interaction

$$V_{DD} = \frac{\sqrt{6}e^2}{R^3}\sum_p C^{20}_{1p1\bar{p}} r_{Ap} r_{B\bar{p}}, \tag{A.2}$$

expressed in a coordinate system with z aligned with $\mathbf{R}$, is symmetric on atom interchange ($A \leftrightarrow B$), the interchange-symmetric state

$$|lml'm'\} \equiv \frac{|(lm)_A(l'm')_B\rangle + |(l'm')_A(lm)_B\rangle}{\sqrt{2(1+\delta_{mm'})}} \tag{A.3}$$

mixes only with the symmetric combinations

$$|l_0 m_0\, l_2 m_2\} \equiv |l_0 m_0\, l_2 m_2 + l_2 m_2\, l_0 m_0\rangle/\sqrt{2}. \tag{A.4}$$

The matrix element of V_{DD} is therefore

$$\{lml m'|V_{DD}|l_1 m_1\, l_2 m_2\} = \frac{\langle lml m'|V_{DD}|l_1 m_1\, l_2 m_2\rangle + (m \leftrightarrow m')}{\sqrt{1+\delta_{mm'}}}. \tag{A.5}$$

We use the Wigner–Eckart theorem to write this explicitly as

$$\{lml m'|V_{DD}|l_1 m_1\, l_2 m_2\} = U_3(R) \sum_p C^{20}_{1p1\bar{p}} \frac{C^{lm}_{l_1 m_1 1 p} C^{lm'}_{l_2 m_2 1\bar{p}} + (2 \leftrightarrow 1)}{(2l+1)\sqrt{(1+\delta_{mm'})/6}} \tag{A.6}$$

where

$$U_3(R) = \frac{e^2 \langle nl||r||n' l_1\rangle \langle nl||r||n'' l_2\rangle}{R^3} \tag{A.7}$$

and the reduced matrix elements are given in terms of radial integrals of r as

$$\langle nl||r||n' l_1\rangle = \sqrt{2l_1+1} C^{l0}_{l_1 010} \int_0^\infty r\, P_{nl}(r)\, P_{n' l_1}(r) \mathrm{d}r. \tag{A.8}$$

For the calculation of matrix elements in this paper, we have used the l-dependent core potentials of Marinescu *et al* [15] and obtained the radial wavefunctions by Numerov integration of the Schrödinger equation. Energy levels were calculated using the recent quantum defect determinations of Li *et al* [16].

A.2. Reflection symmetry

The dipole–dipole matrix element $\{l_0 m_0\, l_0 \bar{m}_0|V_{DD}|l_1 m\, l_2 \bar{m}\}$ is proportional to

$$\sum_p \left(C^{l_0 m_0}_{l_1 m 1 p} C^{20}_{1p1\bar{p}} C^{l_0 \bar{m}_0}_{l_2 \bar{m} 1 \bar{p}} + C^{l_0 m_0}_{l_2 \bar{m} 1 p} C^{20}_{1p\bar{p}} C^{l_0 \bar{m}_0}_{l_1 m 1 \bar{p}}\right)$$

$$= \sum_p \left(C^{l_0 m_0}_{l_1 m 1 p} C^{20}_{1p1\bar{p}} C^{l_0 m_0}_{l_2 m 1 p} + C^{l_0 m_0}_{l_1 \bar{m} 1 p} C^{20}_{1p\bar{p}} C^{l_0 m_0}_{l_2 \bar{m} 1 p}\right) \tag{A.9}$$

where the Clebsch–Gordan symmetry $C^{c\gamma}_{a\alpha b\beta} = -1^{a+b-c} C^{c\bar{\gamma}}_{a\bar{\alpha} b\bar{\beta}}$ has been used along with the specific parities $(-1)^{l_1} = (-1)^{l_2} = -(-1)^{l_0}$. Inspection of equation (A.9) then shows that

$$\{l_0 m_0\, l_0 \bar{m}_0|V_{DD}|l_1 m\, l_2 \bar{m}\} = \{l_0 m_0\, l_0 \bar{m}_0|V_{DD}|l_1 \bar{m}\, l_2 m\}. \tag{A.10}$$

References

[1] Lukin M D, Fleischhauer M, Cote R, Duan L M, Jaksch D, Cirac J I and Zoller P 2001 Dipole blockade and quantum information processing in mesoscopic atomic ensembles *Phys. Rev. Lett.* **87** 037901

[2] Föster T 1996 *Modern Quantum Chemistry* ed O Sinanoglu (New York: Academic)

[3] Fioretti A, Comparat D, Drag C, Gallagher T F and Pillet P 1999 Long-range forces between cold atoms *Phys. Rev. Lett.* **82** 1839

[4] Hettich C, Schmitt C, Zitzmann J, Kuhn S, Gerhardt I and Sandoghdar V 2002 Nanometer resolution and coherent optical dipole coupling of two individual molecules *Science* **298** 385

[5] Peil S, Porto J V, Tolra B L, Obrecht J M, King B E, Subbotin M, Rolston S L and Phillips W D 2003 Patterned loading of a Bose–Einstein condensate into an optical lattice *Phys. Rev.* A **67** 051603(R)

[6] Sebby-Strabley J, Newell R T R, Day J O, Brekke E and Walker T G 2004 High density mesoscopic atom clouds in a holographic atom trap *Preprint* physics/0408028

[7] Saffman M and Walker T G 2002 Engineering single atom and single photon sources from entangled atomic ensembles *Phys. Rev.* A **66** 065403

[8] Saffman M and Walker T G 2004 Entangling single and N atom qubits for fast quantum state detection and transmission *Preprint* quant-ph/0402111
[9] Tong D, Farooqi S, Stanojevic J, Krishnan S, Zhang Y, Cote R, Eyler E and Gould P 2004 Local blockade of Rydberg excitation in an ultracold gas *Phys. Rev. Lett.* **93** 063001
[10] Singer K, Reetz-Lamour M, Amthor T, Marcassa L G and Weidemüller M 2004 Suppression of excitation and spectral broadening induced by interactions in a cold gas of Rydberg atoms *Phys. Rev. Lett.* **93** 163001
[11] Protsenko I E, Reymond G, Schlosser N and Grangier P 2002 Operation of a quantum phase gate using neutral atoms in microscopic dipole traps *Phys. Rev.* A **65** 052301
[12] Ryabtsev I I, Tretyakov D B and Beterov I I 2004 Applicability of Rydberg atoms to quantum computers *Preprint* quant-ph/0402006
[13] Marinescu M 1997 Dispersion coefficients for the *n*P–*n*P asymptote of homonuclear alkali–metal dimers *Phys. Rev.* A **56** 4764
[14] Boisseau C, Simbotin I and Cote R 2002 Macrodimers: ultralong range Rydberg molecules *Phys. Rev. Lett.* **88** 133004
[15] Marinescu M, Sadeghpour H R and Dalgarno A 1994 Dispersion coefficients for alkali-metal dimers *Phys. Rev.* A **49** 982
[16] Li W, Mourachko I, Noel M W and Gallagher T F 2003 Millimeter-wave spectroscopy of cold Rb Rydberg atoms in a magneto-optical trap: quantum defects of the *n*s, *n*p, and *n*d series *Phys. Rev.* A **67** 052502